Biomedicine & Pharmacotherapy 192 (2025) 118643

Contents lists available at ScienceDirect

Biomedicine & Pharmacotherapy

journal homepage: www.elsevier.com/locate/biopha

Boosting curcumin derivatives' cytotoxicity in cancer cells with light: An *in vitro* study

Giulia Greco [a], Eleonora Turrini [b], Fabio Ferrini [c], Francesca Maffei [b], Giulia Neggiani [b], Matteo Calvaresi [a,d], Manuele Di Sante [a,d], Matteo Di Giosia [a,d], Federica Belluti [e], Piero Sestili [c,1], Carmela Fimognari [b,*,1]

[a] Department of Chemistry Giacomo Ciamician, Alma Mater Studiorum – University of Bologna, Via Piero Gobetti 85, Bologna 40129, Italy
[b] Department for Life Quality Studies, Alma Mater Studiorum – University of Bologna, Corso D'Augusto 237 Rimini 47921, Italy
[c] Department of Biomolecular Sciences, University of Urbino Carlo Bo, Via I Maggetti 26, Urbino 61029, Italy
[d] IRCCS Azienda Ospedaliero - Universitaria di Bologna, Laboratory of Preclinical and Translational Research in Oncology (PRO), Bologna 40138, Italy
[e] Department of Pharmacy and Biotechnology, Alma Mater Studiorum – University of Bologna, Via Belmeloro 6, Bologna 40126, Italy

ARTICLE INFO

Keywords:
Photodynamic therapy
Photosensitizers
Curcumin derivatives
Cytotoxicity
Apoptosis
Ferroptosis

ABSTRACT

Curcumin is a natural compound with well-documented anticancer potential, but its clinical use is limited by poor water solubility and low bioavailability. To address these limitations, various nanoformulations and synthetic or semi-synthetic derivatives have been developed. Due to its ability to absorb visible light, curcumin has also been investigated as a natural photosensitizer (PS) for photodynamic therapy (PDT), a therapeutic approach that utilizes light-activated compounds to kills cancer cells by ROS generation. This study investigates the photosensitizing, cytotoxic, and phototoxic effects of three novel curcumin derivatives (AP2961, AP2962, and AP2975) in HL-60 and MCF-7 cancer cells and characterize the underlying mechanisms. As shown by flow cytometry within the SYTOX™ red probe, exposure to a low-irradiance white LED light significantly increased the cytotoxicity of our derivatives in both cell lines, with AP2975 being the most effective, especially in HL-60 cells. Photoactivated AP2975 produced peroxides ROS via type I mechanism; colorimetric as well as fluorimetric assays showed that it depleted intracellular glutathione and inhibited catalase activity, thus inducing oxidative stress. Additionally, AP2975 triggered i) apoptosis, as demonstrated by the partial recovery of cell viability observed with zVAD, Annexin-V assay, and increase in PARP cleavage, ii) ferroptosis as confirmed by the partial recovery of cell viability recorded with ferrostatin-1 and decrease in GPX4 expression, and iii) necrosis, as recorded by Annexin-V assay. Overall, AP2975 may represent a promising PS for PDT, thanks to its combined pro-apoptotic and pro-ferroptotic activity, and emerges as a good candidate for future *in vivo* studies.

1. Introduction

Phytochemicals are naturally occurring bioactive substances present in a wide variety of plant-based foods such as fruits, vegetables, and cereals. The dietary intake of these compounds is associated with the mitigation of numerous health conditions, including cardiovascular and neurodegenerative diseases, diabetes, immunological disorders, and cancer [1]. Multiple clinical and epidemiological studies have reported inverse correlations between the consumption of certain phytochemicals and cancer incidence and recurrence [2–4]. This protective effect is largely attributed to their ability to interfere with multiple molecular pathways involved in carcinogenesis [2]. As a result, phytochemicals have drawn considerable attention for their potential role as anticancer agents [4].

Curcumin, the major biologically active constituent of the rhizome of *Curcuma longa* (turmeric) [5], is among the most extensively studied phytochemicals. It has been used for centuries in Ayurveda, Unani, and traditional Chinese medicine to treat various conditions [5]. Since the

* Corresponding author.
E-mail addresses: giulia.greco9@unibo.it (G. Greco), eleonora.turrini@unibo.it (E. Turrini), fabio.ferrini@uniurb.it (F. Ferrini), francesca.maffei@unibo.it (F. Maffei), giulia.neggiani2@unibo.it (G. Neggiani), matteo.calvaresi3@unibo.it (M. Calvaresi), manuele.disante2@unibo.it (M. Di Sante), matteo.digiosia2@unibo.it (M. Di Giosia), federica.belluti@unibo.it (F. Belluti), piero.sestili@uniurb.it (P. Sestili), carmela.fimognari@unibo.it (C. Fimognari).
[1] Co-last authors.

https://doi.org/10.1016/j.biopha.2025.118643
Received 23 August 2025; Received in revised form 18 September 2025; Accepted 4 October 2025
Available online 9 October 2025

1950s, numerous preclinical studies and clinical trials have confirmed its broad spectrum pharmacological properties, including anti-inflammatory [6–8], analgesic [7,8], antioxidant [8–10], antiviral [11], and antimicrobial effects [11]. This polyphenol also exhibits a multifaceted cancer chemopreventive and chemotherapeutic activity through multiple mechanisms. Specifically, it was shown to impede or delay the early stages of carcinogenesis due to its antioxidant and anti-inflammatory properties, along with its ability to modulate the activities of metabolizing enzymes [3,10]. Curcumin also showed an anticancer potential by inducing oxidative stress, apoptosis, autophagy, cell-cycle arrest, and by acting as an epigenetic and micro-ribonucleic acids (miRNAs) modulator [3,10,12,13]. Additionally, it has been shown to enhance the sensitivity of cancer cells to common chemotherapy agents, such as doxorubicin, cisplatin, paclitaxel, and 5-fluorouracil [14]. Along with its pleiotropic anticancer activity, curcumin has been demonstrated to be safe and to have high tolerability, as its administration at doses of up to 12 g per day caused no adverse effects in clinical trials [8,15–17]. Nevertheless, curcumin's clinical use is limited by a poor bioavailability, due to low intestinal absorption, rapid metabolism, and poor water solubility [18]. To address these challenges, several strategies have been proposed, including the inclusion of curcumin in nanoformulations [19,20] and the synthesis or semi-synthesis of structurally related analogues [21]. Proper chemical modifications and functionalisation of the curcumin backbone have successfully enabled the design of agents that can effectively and selectively modulate well-defined targets and biochemical pathways involved in various pathologies, such as cancers and neurodegeneration. This demonstrates the value of this strategy, as evidenced by the numerous articles on this topic [22–27]. In this context, our research group recently published data on newly synthesized curcumin analogues, obtained by incorporating a substituted benzyl-1,2,3-triazole unit into different positions of the curcumin scaffold. This design strategy aimed to enhance the bioavailability and anticancer profile of the analogues, thereby increasing cytotoxicity that resulted in up to threefold greater activity than that of curcumin against T acute lymphoblastic leukaemia cells [28].

Photodynamic therapy (PDT) is an approved therapeutic approach for treating various cancer types based on the production of reactive oxygen species (ROS) triggered by the light exposure of photoactive compounds, known as photosensitizers (PSs) [29]. Curcumin possesses inherent photosensitizing properties, as it can absorb UV–visible light in the 300–500 nm spectral range [30], suggesting that it potentially serves as a natural PS for PDT. In this regard, *in vitro* and *in vivo* studies have demonstrated that light irradiation enhances the cytotoxic effects of curcumin [18,30–32]. Therefore, building on the promising anticancer potential of the new curcumin analogues previously published by our research group, in this work we aimed to determine whether AP2961, AP2962, and AP2975, previously referred as compound 4, 2, and 3, respectively [28], possess photosensitizing properties, using curcumin as a reference standard. The compounds were selected based on their cytotoxic potency: low (AP2961), mild (AP 2962), and high (AP2975) after 24 h of treatment. In particular, we investigated their phototoxic potential on human acute promyelocytic leukaemia (HL-60) and estrogen and progesterone receptor-positive human breast cancer (MCF-7) cells and the underlying molecular mechanisms.

2. Materials and methods

2.1. Cell cultures

HL-60 and MCF-7 cells were obtained from ATCC (LGC Group, Middelsex, UK) and cultured in RPMI 1640 supplemented with 20 or 10 %, respectively, heat inactivated foetal bovine serum (FBS), 1 % L-glutamine 200 mM, and 1 % penicillin/streptomycin solution 100 U/mL (all obtained from Euroclone, Pero, MI, Italy). Cells were maintained in culture in a humidified incubator with 5 % of CO_2. To maintain exponential growth, HL-60 cells were cultured without never exceeding their maximal density of 1×10^6/mL, while MCF-7 cells were trypsinised upon reaching 70–80 % confluence.

2.2. Cell treatment and irradiation

To compare the cytotoxic effects of curcumin and of its derivatives AP2961, AP2962 or AP2975 after light irradiation or dark incubation, HL-60 and MCF-7 cells were treated with increasing concentration of curcumin, AP2961, AP2962 or AP2975 (0–100 μM) for 4 h. After incubation, cells were washed twice with phosphate buffered saline (PBS) 1X and irradiated in PBS 1X for 30 min with a low-irradiance white light LED (24 mW/cm^2) or kept in dark. Following irradiation or dark incubation, PBS was withdrawn, and cells were cultured in drug-free complete medium for 1, 24, or 48 h depending on experimental exigencies.

2.3. Analysis of cell viability

HL-60 cells were seeded at a density of 0.25×10^6/mL and treated as previously described. Cell viability was assessed by flow cytometry using the cell-impermeant fluorescent probe SYTOX™ red (Thermo Fisher Scientific, Waltham, MA, USA). This probe can exclusively bind the DNA of cells within damaged cell membrane, thus emitting a fluorescent signal that is inversely proportional to cell viability. Briefly, after 48 h of recovery in drug-free complete medium, cells were diluted in PBS 1X containing SYTOX™ red (5 nM), incubated at room temperature for 20 min and then analysed by flow cytometry using a Guava EasyCyte 6 2 L cytometer (Guava Technologies, Merck Millipore, Darmstadt, Germany).

For MCF-7 cells, 10000 cells in 100 μL complete medium were seeded in 96 well plate and the day after treated as described above. After light exposure or dark incubation and recovery in drug-free complete medium for 48 h, cell viability was assessed using the colorimetric MTT (3-(4,5-dimethylthiazol-2-yl)-2,5-diphenyltetrazolium bromide, Merck, St. Luis, MO, USA) assay. Briefly, cells were incubated for 90 min at 37°C in medium containing 0.5 mg/mL of MTT. After incubation, MTT solution was removed, and the formazan salts generated by living cells were solubilized by adding dimethyl sulfoxide (DMSO). The absorbance, which is proportional to cell viability, was recorded at a wavelength of 570 nm using the Victor X3 multilabel plate reader (Perkin Elmer, Waltham, MA, USA).

For both cell lines, the percentage (%) of viable cells was normalized to that of untreated cells and IC_{50} values (concentrations that inhibit 50 % of cell viability) were calculated from the dose–response curve.

2.4. Quantification of reactive oxygen species (ROS) in cell-free model

The Amplex Red assay was used to evaluate the ability of AP2975 to generate hydrogen peroxide (H_2O_2), the most thermodynamically stable product originated following the type I ROS reaction mechanism. Amplex Red (10-acetyl-3,7-dihydroxyphenoxazine; AR) is a colourless and nonfluorescent molecule. In the presence of H_2O_2 and horseradish peroxidase (HRP), AR is oxidized to form resorufin, a highly fluorescent compound. Due to its high sensitivity, this assay provides an estimation of the PDT efficiency, related to the type I mechanism. Using a calibration curve determined with standard solutions of H_2O_2, it is possible to estimate the quantity of H_2O_2 generated from the fluorescence intensity of resorufin [33–38]. 10 μL of AR (50 mM in DMSO) and 10 μL of HRP (0.4 mg/mL in 50 mM PBS at pH 7.4) were added to 1 mL of PBS to obtain the final working solution. In a 96-well plate, 85 μL of PBS were placed in each well, and then 5 μL of AP2975 stock solutions (1, 2, 5, 10, 20 μM in DMSO) were added. The plate was irradiated with a low-irradiance white light LED (24 mW/cm^2) for 30 min and then 10 μL of the working solution were added to each well. An identical plate was kept in the dark before the addition of the working solution. After 30 min of rest, the fluorescence intensity recorded at 590 nm (excitation:

560 nm) was collected using a PerkinElmer EnSpire® Multimode Plate Reader (PerkinElmer).

ABMDMA (9,10-anthracenediyl-bis(methylene) dimalonic acid) is a molecular probe used for the detection and quantification of singlet oxygen ($^1O_2$) produced following the type II PDT mechanism. The assay is highly selective for singlet oxygen ($^1O_2$), showing minimal interference from other ROS, so it can be used for assessing type II PDT efficiency. ABMDMA is a fluorescent molecule that reacts selectively with $^1O_2$ to form a non-fluorescent endoperoxide. During reaction with singlet oxygen ($^1O_2$), ABMDMA exhibits a measurable decrease in its absorbance. A stock solution of AP2975 (76.481 mM) was prepared in PBS containing 5 % DMSO. Working solutions at concentrations of 1, 2, 5, 10, 20 μM were obtained by dilution in PBS, prepared with D_2O to prevent $^1O_2$ quenching. For the assay, 97 μL of each AP2975 solution were dispensed into wells of a 96-well plate, followed by the addition of 3 μL of a 5 mM ABMDMA stock solution (prepared in DMSO), yielding a final ABMDMA concentration of 150 μM. The plate was then irradiated for 30 min using a low-irradiance white light LED (24 mW/cm^2). Absorbance readings were collected at 380 nm before and after irradiation using an EnSpire® Multimode Plate Reader. The amount of $^1O_2$ generated upon irradiation was quantified based on the decrease in ABMDMA absorbance.

2.5. Analysis of intracellular ROS generation

HL-60 cells were seeded at a density of 0.25×10^6/mL and pre-treated for 1 h with the iron chelator 1,10-phenanthroline (*o*-phen, 5 μM, Merck), the antioxidant trolox (1 mM, Santa Cruz Biotechnologies, Dallas, TX, USA), the ROS scavengers butylated hydroxytoluene (BHT, 3 μM, Santa Cruz Biotechnologies) and N-acetyl-L-cysteine (NAC, 5 mM, Santa Cruz Biotechnologies), the mitochondrial complex I inhibitor rotenone (ROT, 0.5 μM, Merck), the glutathione (GSH) depletor L-buthionine-S,R-sulfoximine (BSO, 200 μM, Santa Cruz Biotechnologies), or for 12 h with the catalase inhibitor 3-amino-1,2,4-triazole (ATZ, 10 mM, Santa Cruz Biotechnologies). After pre-treatment, cells were exposed to AP2975 (5 or 10 μM) for 4 h and irradiated for 30 min. At the end of irradiation, cells were cultured for 24 h in medium containing the corresponding antioxidants or pro-oxidants and cell viability was analyzed by flow cytometry with SYTOX™ red as described above.

2.6. Measurement of intracellular reduced glutathione

The intracellular GSH levels were quantified using Ellman's reagent [5,5′-dithiobis-(2-nitrobenzoic acid), DTNB]. Briefly, after 1 or 24 h of recovery, HL-60 cells were collected, washed with PBS 1x, and lysed using CelLytic™ reagent (Merck). Protein concentration in each sample was determined via the Bradford assay, using a bovine serum albumin standard curve for quantification. For each sample, an equal amount of proteins was used to assess GSH levels. Cell lysates were deproteinized with trichloroacetic acid, followed by centrifugation at 14.000 rpm for 5 min to remove precipitated proteins. A 50 μL aliquot of the resulting supernatant was combined with Tris-EDTA buffer (pH 8.9) and DTNB solution (0.01 M in methanol). DTNB reacts with the free thiol groups of GSH to generate a yellow chromophore, 2-nitro-5-thiobenzoic acid, alongside glutathione disulfide (GSSG) [39]. This reaction product was detected at 405 nm using an Infinite® F200 PRO microplate reader (Tecan, Männedorf, Switzerland). GSH content was expressed as fold change compared to control. NAC (5 mM) and BSO (200 μM) were included as positive controls for assay validation.

2.7. Measurement of catalase activity

HL-60 cells were pre-treated or not with ATZ 10 mM for 12 h, then exposed to AP2975 (5 or 10 μM) for 4 h and irradiated for 30 min. After 24 h of recovery in ATZ-containing medium, cells were collected and catalase activity was determined spectrophotometrically in cell homogenates with the methods of Aebi [40]. Briefly, cells were washed twice with PBS and scraped into 5 mM KH_2PO_4/Na_2HPO_4 buffer (containing 3 mM KF and 3 mM β-mercaptoethanol, pH 7.5). Then, the resulting suspension was sonicated three times with 10-second pulses and centrifuged at 12.000 × g for 10 min at 4°C. To stabilize the lysate, ethanol was added to the supernatant to degrade the 'complex II' of catalase along with H_2O_2. Following this step, 50 μl of 1 M Tris-HCl, 5 mM EDTA (pH 8.0), 450 μl of H_2O_2, and 450 μl of H_2O were added. The reaction was incubated at 37°C for 10 min; after that, the sample was introduced, and the catalase activity was assessed spectrophotometrically by observing the reduction in absorbance at 230 nm due to the depletion of H_2O_2. One unit of catalase activity is defined as the decomposition of 1 μmol of H_2O_2 per minute under the specified assay conditions ($\varepsilon 230 = 0.071$). Catalase activity was reported as U/mg of proteins.

2.8. Analysis of cell death mechanism

HL-60 cells were treated with AP2975 and exposed to light irradiation as previously described. After recovery in complete drug-free medium for 24 or 48 h, cells were diluted with Guava Nexin Reagent (Luminex, Austin, TX, USA) containing the cell-impermeant fluorescent dye 7-aminoactinomycin D (7- AAD) and Annexin V-phycoerythrin and analyzed via flow cytometry. Annexin V binds phosphatidylserine, which translocates from the inner to the outer side of the membrane of cells in early phases of programmed cell death (PCD; *i.e.*, apoptosis, ferroptosis, or necroptosis) [41]. Since the inner PS can be bound by Annexin-V even in cells within damaged cell membranes (*i.e.*, cells in the later stages of PCD or necrotic cells), the cell-impermeant fluorophore 7-AAD contained in the reagent serves as a membrane integrity marker. Then, flow cytometry analysis distinguishes three cell populations: viable cells (Annexin V^-/7-AAD^-), cells undergoing cell death in the early stages of PCDs (Annexin V^+/7-AAD^-), cells in the late cell death stages of PCD or necrotic cells (Annexin V^+/7-AAD^+).

To characterize the mechanism of cell death, HL-60 cells were pre-treated for 1 h with or without different inhibitors: the pan-caspase inhibitor carbobenzoxy-valyl-alanyl-aspartyl-[O-methyl]-fluoromethylketone (zVAD-fmk, 50 μM, Selleckchem, Houston, TX, USA) that blocks apoptosis; the inhibitors of lipidic ROS and lipid peroxidation ferrostatin-1 (Fer-1, 1 μM, Merck) or vitamin E (vit E, 100 μM, Merck), the iron chelator deferoxamine (DFO, 10 μM, Acros Organics, Thermofisher Scientific, Geel, Belgium) that inhibit ferroptosis; the RIPK1 inhibitor necrostatin-1s (Nec-1s, 75 μM, Merck) that blocks necroptosis. After pre-treatment with the different inhibitors, cells were exposed to AP2975 (10 μM) for 4 h and irradiated for 30 min. At the end of irradiation, cells were cultured for 24 or 48 h in medium containing the cell death inhibitors and cell viability was analyzed by flow cytometry with SYTOX™ red, as described above.

2.9. Analysis of cleaved PARP1 [poly (ADP-ribose) polymerase] and GPX4 (glutathione peroxidase 4) protein expression

After 24 or 48 h of recovery in drug-free complete medium, about 1×10^6 HL-60 cells were collected, washed in PSB 1X, fixed in 4 % paraformaldehyde and permeabilized using 90 % cold methanol. Then, cells were incubated first with the primary anti-PARP1 (cleaved Asp214) antibody (0.25 μg/test; no. MA5–37112, Invitrogen, Thermo Fisher Scientific) or the primary anti-GPX4 antibody (1:150; no. PA5–109274, Invitrogen, Thermo Fisher Scientific) for 1 h at room temperature and then incubated with Alexa Fluor 647-labeled secondary antibody (1:200, no. A21244, Invitrogen) for 45 min at room temperature. Finally, cells were washed and analyzed by flow cytometry. Protein expression of cleaved PARP was expressed as % of positive cells, while GPX4 protein expression was expressed as the fold change of the mean fluorescence intensity (MFI) of treated samples compared to untreated cells.

2.10. Statistical analysis

All results are expressed as mean ± SEM or SD of at least three independent experiments. Statistical analyses were performed using one- or two-way ANOVA, and Tukey, Dunnet or Bonferroni as post-tests. IC_{50} values were calculated from the dose–response curve using the non-linear regression [log(inhibitor) versus normalized response]. The statistical software GraphPad InStat 9.0 version (GraphPad Prism, San Diego, CA, USA) was used, and $p < 0.05$ was considered significant.

3. Results

3.1. Light irradiation enhances the cytotoxic effects of curcumin's derivatives on both HL-60 and MCF-7 cells

The compounds tested in this study are part of a series of curcumin-based analogues previously tested on T acute lymphoblastic leukaemia cells (CCRF–CEM), which demonstrated different cytotoxic potency depending on the specific functionalization of the curcumin scaffold [28]. In the present study, curcumin, AP2961, AP2962 and AP2975 showed cytotoxic effects on both HL-60 and MCF-7 cells, with varying potencies across the two cell lines. In HL-60 cells, AP2962 exhibited the greatest cytotoxic activity, markedly higher than that of curcumin, while AP2961 and AP2975 demonstrated lower efficacy, far less potent than curcumin (Fig. 1 and Table 1). In MCF-7 cells, AP2961 and AP2962 displayed cytotoxic effects comparable to curcumin, while AP2975 was less active (Fig. 1 and Table 1).

Taking into account the ability of the curcuminoid scaffold to absorb visible light and thereby to serve as potential PSs for PDT [30], we assessed the cytotoxic activity of curcumin and the three curcumin-based derivatives upon exposure to light irradiation. The photoactivation significantly increased the cytotoxicity of the tested analogues (Fig. 1), and among them, AP2975 showed the strongest

Table 1
IC_{50} values, calculated after incubation with curcumin or its derivatives AP2961, AP2962, or AP2975 for 4 h followed or not by 30 min light irradiation and 48 h recovery in drug-free complete medium, and relative phototoxicity index factor (PIF), calculated dividing dark IC_{50} [*: extrapolated from dose-response curves (drug concentration versus cell viability)] by light IC_{50} values.

	HL-60			MCF-7		
	IC_{50} (μM)		PIF	IC_{50} (μM)		PIF
	Dark	Light		Dark	Light	
AP2961	> 100	3.24	96.51*	59.16	4.86	12.17
AP2962	6.77	5.51	1.23	40.71	4.80	8.48
AP2975	> 100	4.11	2228.47*	> 100	6.25	55.41*
Curcumin	38.41	5.78	6.65	44.94	4.71	9.54

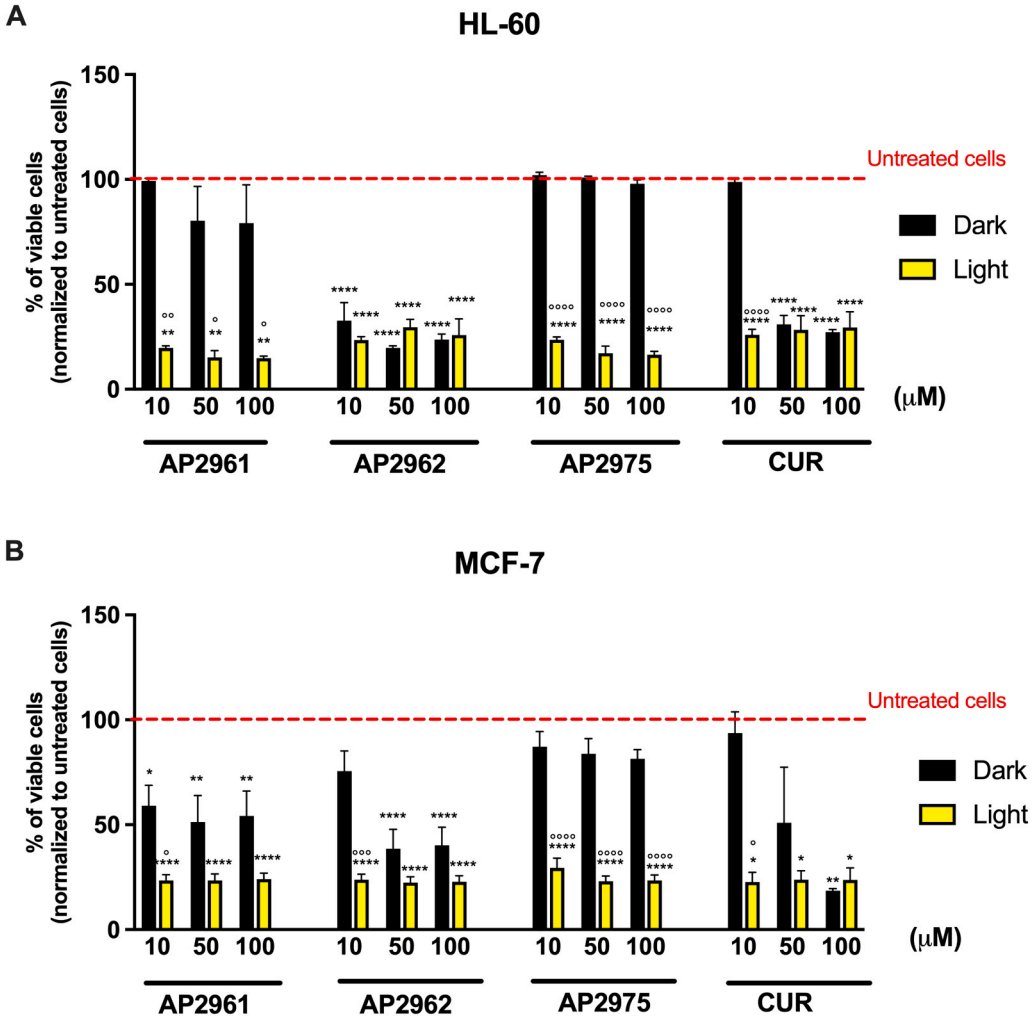

Fig. 1. Photoactivation potentiates the cytotoxicity of curcumin and its analogues. Percentage (%) of HL-60 (A) and MCF-7 (B) viable cells after exposure to the curcumin derivatives or curcumin (CUR) for 4 h followed or not by 30 min light irradiation and 48 h recovery in drug-free complete medium. * $p < 0.05$; ** $p < 0.01$; **** $p < 0.0001$ versus untreated cells. ° $p < 0.05$; °° $p < 0.01$; °°° $p < 0.001$; °°°° $p < 0.0001$ versus non-irradiated cells.

phototoxic effect (Fig. 1), especially in HL-60 cells, with a phototoxic index factor (PIF, defined as the IC_{50} in the dark divided by the IC_{50} under irradiation) exceeding 2000, far surpassing that of curcumin (6.65, Table 1). AP2975 also outperformed curcumin in light-induced cytotoxicity on MCF-7 cells, achieving a PIF value equivalent to 55.41, which is 5.81 times higher than the 9.54 calculated for curcumin (Table 1). Taken together, these findings indicate that this analogue exhibits a strong light-dependent cytotoxicity in cancer cells, considerably greater than that of curcumin, especially in HL-60 cells, where the best PIF value was recorded. Based on these results, AP2975 was deeply studied to characterize the molecular mechanisms underlying the phototoxic effects on HL-60 cells.

3.2. Photoactivated AP2975 generates peroxides following type I PDT mechanism and promotes oxidative stress

Measuring ROS generated by a PS is crucial to evaluate its effectiveness. Two *in vitro* assays are commonly used to detect ROS generated by the type I mechanism (Amplex Red assay) or the type II mechanism (ABMDMA assay).

The results of the two cell-free assays showed that AP2975, upon irradiation, can generate peroxides (*via* the type I mechanism) in a concentration-dependent manner: from 113.4 nM at 5 μM to 295 nM at the highest tested 20 μM concentration (Fig. 2A). On the contrary, the type II mechanism is inactive (data not shown).

Then, we explored whether photoactivated AP2975 could increase the levels of intracellular ROS. Thus, we investigated the capacity of antioxidant (NAC, trolox, *o*-phen, BHT) or prooxidant (BSO, ATZ) preconditioning to modulate the cytotoxic response of HL-60 cells exposed to photoactivated AP2975. The addition of BHT, NAC or *o*-phen caused a significant protection from AP2975 toxicity (Fig. 2B). NAC also increased the intracellular levels of thiols (-SH), suggesting that its effect may result from both direct scavenging of ROS and from serving as a thiol donor for the glutathione peroxidase/reductase (GpX/GR) pathway (Fig. 2C). Along this line, depletion of intracellular thiols caused by BSO markedly increased HL-60 cell death (Fig. 2B). Interestingly, inhibition of catalase with ATZ pre-treatment did not modify the cytotoxic response (Fig. 2B). Similarly, no effect was found on incubating cells in the presence of rotenone, an inhibitor of the Complex I of the mitochondrial respiratory chain (Fig. 2B).

3.3. AP2975 promotes apoptotic, ferroptotic, and necrotic cell death upon irradiation

In order to elucidate the mechanisms of cell death triggered by photoactivated AP2975, we first performed the Annexin-V assay. When irradiated, AP2975 caused a concentration- and time-dependent increase in cells in early stages of PCD (Annexin-V^+/7-AAD^-), reaching 36.6 % and 69.6 % at 24 and 48 h, respectively, at the highest tested concentration of 10 μM (Fig. 3A). Besides, a concentration-dependent increase in Annexin-V^+/7-AAD^+ cells was also observed, indicative of later stages of PCD or necrosis (Fig. 3A).

Since PS exposure is common to multiple PCD pathways [41], we next characterized which of these was triggered by photoactivated AP2975. HL-60 cells pre-treated with the pan-caspase inhibitor zVAD showed a significant recovery of cell viability compared to that of cells

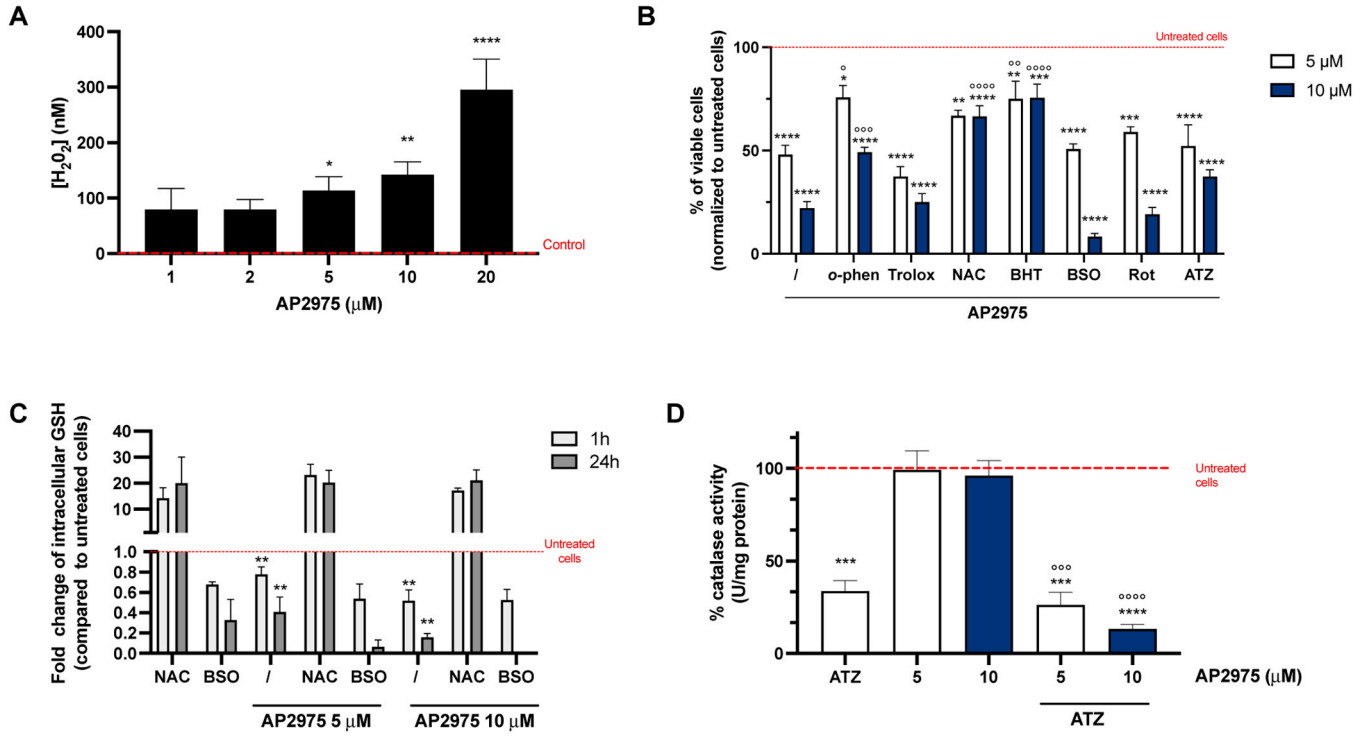

Fig. 2. Photoactivated AP2975 generates peroxides via type I PDT mechanism and promotes intracellular oxidative stress. A. Quantification of ROS generated through type I mechanism as a function of AP2975 concentration after 30 min of white light irradiation, using the Amplex Red assay. **B.** Percentage (%) of viable HL-60 cells following 1 h pre-treatment with 1,10-phenanthroline (*o*-phen), Trolox, N-acetyl-L-cysteine (NAC), butylated hydroxytoluene (BHT), L-buthionine-S,R-sulfoximine (BSO), rotenone (Rot), or 12 h pre-treatment with 3-amino-1,2,4-triazole (ATZ), then a 4 h treatment with AP2975 (5 and 10 μM), 30 min of irradiation with white LED light, and a 24 h recovery in culture medium containing the respective antioxidant or pro-oxidant agents. **C.** Levels of intracellular reduced GSH in HL-60 cells pre-treated or not for 1 h with NAC (5 mM) or BSO (200 μM), exposed to AP2975 (5 and 10 μM) for 4 h, irradiated with white LED light for 30 min and recovered for 1 or 24 h in NAC- or BSO-containing medium. **D.** Catalase activity (expressed as % of U/mg protein compared to untreated cells) in HL-60 cells pre-treated or not for 12 h with ATZ 10 mM, exposed to AP2975 (5 and 10 μM) for 4 h, irradiated with white LED light for 30 min and recovered for 24 h in ATZ-containing medium. * $p < 0.05$; ** $p < 0.01$; *** $p < 0.001$; **** $p < 0.0001$ versus untreated cells or AP2975 0 μM. ° $p < 0.05$; °° $p < 0.01$; °°° $p < 0.001$; °°°° $p < 0.0001$ versus cells treated with AP2975.

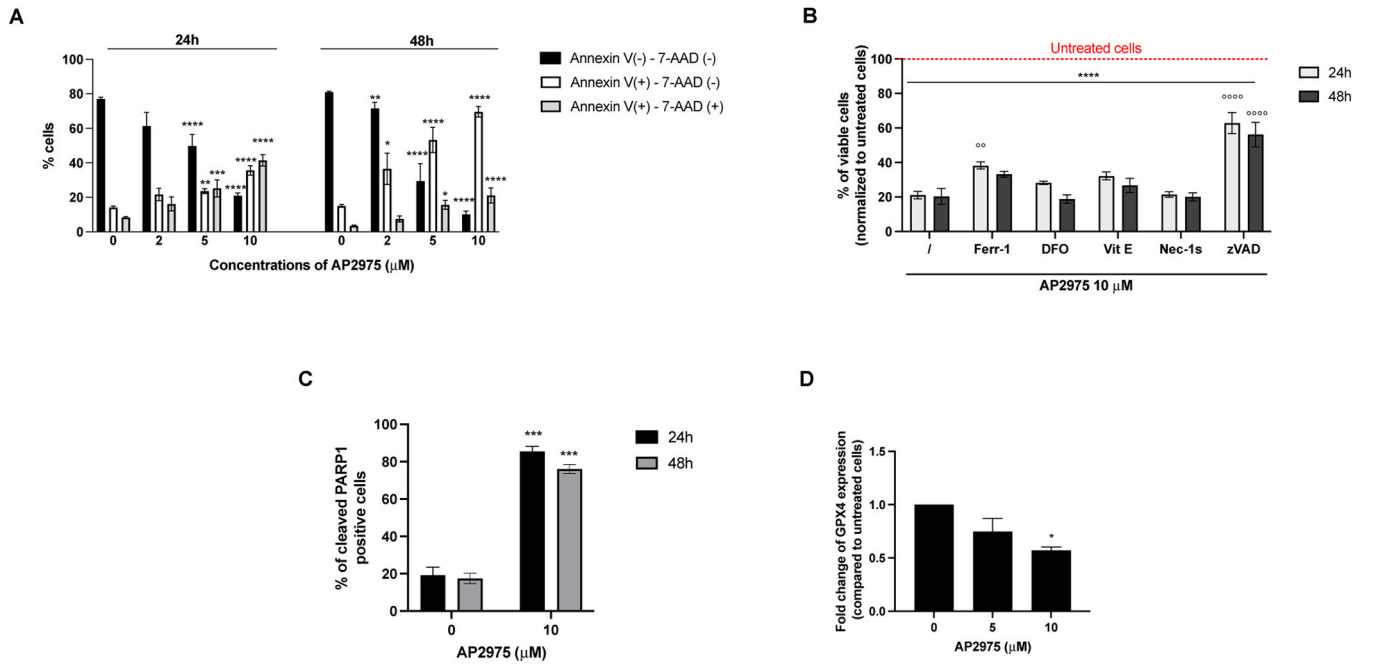

Fig. 3. Photoactivated AP2975 induces apoptosis, ferroptosis, and necrosis. A. Percentage (%) of HL-60 Annexin V^-/7-AAD^-, Annexin V^+/7-AAD^-, Annexin-V^+/7-AAD^+ cells after exposure to AP2975 for 4 h followed by 30 min light irradiation and 24- or 48-hours recovery in drug-free complete medium. **B.** % of HL-60 viable cells following a 1 h pre-treatment with ferrostatin-1 (Ferr-1, 1 μM), deferoxamine (DFO, 10 μM), vitamin E (Vit E, 100 μM), necrostatin-1s (Nec-1s, 75 μM), and carbobenzoxy-valyl-alanyl-aspartyl-[O-methyl]-fluoromethylketone (zVAD, 50 μM), 4 h treatment with AP2975 10 μM followed by 30 min light exposure and 24 or 48 h recovery in inhibitors-containing complete medium. **C.** % of HL-60 cells positive for cleaved PARP1 after 4 h treatment with AP2975 10 μM, 30 min light exposure and 24 or 48 h recovery in drug-free complete medium. **D.** GPX4 protein expression (fold change) in HL-60 cells treated for 4 h with AP2975 (5 and 10 μM), 30 min light exposure and 24 h recovery in drug-free complete medium. * $p < 0.05$; ** $p < 0.01$; *** $p < 0.001$; **** $p < 0.0001$ versus untreated cells; °° $p < 0.01$; °°°° $p < 0.0001$ versus AP2975-treated cells.

only treated with AP2975: 62.81 % versus 21.11 % at 24 h and 56.18 % versus 20.4 % at 48 h (Fig. 3B). The caspase-dependent cleavage of PARP1 is widely recognized as a hallmark of apoptotic cell death [42], therefore we measured the expression of cleaved PARP1 to confirm the involvement of apoptosis. Photoactivated AP2975 increased the percentage of PARP1-cleaved positive cells to 85.6 % (versus 19.2 % in untreated controls) after 24 h, and to 76.1 % (versus 17.5 %) after 48 h of recovery from treatment (Fig. 3C). Alongside apoptosis, we identified the involvement of ferroptosis, a lipid peroxidation-driven cell death mechanism primarily resulting from diminished GPX4 activity, which normally mitigates oxidative damage by utilizing GSH to detoxify lipid peroxides [43]. Indeed, although to a lesser extent compared to the apoptosis inhibitor, Ferr-1 significantly restored cell viability 24 h after irradiation (38.25 % versus 21.11 % in AP2975-treated cells) (Fig. 3B). Additionally, along with the previously described intracellular GSH depletion (Fig. 2C), AP2975 significantly reduced the protein expression of GPX4 in a concentration-dependent manner (by 25 % at 5 μM and by 43 % at 10 μM) (Fig. 3D).

Overall, our data indicate that photoactivated AP2975, after 24 h from irradiation, triggers multiple cell-death pathways, including apoptosis, ferroptosis, and necrosis, while after 48 h cells undergo apoptosis and necrosis exclusively.

4. Discussion

Curcumin derivatives AP2961, AP2962, and AP2975 induced significant cytotoxic effects in both HL-60 and MCF-7 cells. These results are in line with our previous findings [28], which reported the cytotoxic effects of these derivatives on T acute lymphoblastic leukemia CCRF-CEM cells, although under different exposure conditions (4 h plus 48 h of recovery versus 24 or 48 h of continuous treatment). In our previous work, the analogue with an unmodified curcumin scaffold and a functionalized triazole in the C-4 central position, such as compound 2, here as AP2962, showed the highest cytotoxic activity after 48 h of treatment [28]. Consistently, we found that this compound also displayed marked cytotoxic effects in dark conditions. On the contrary, a loss of activity was observed for AP2961 and AP2975, both characterized by a substituted benzyl-triazole in a side ring of curcumin [28]. This behaviour may confirm that combining the 1,2,3-triazole-based synthon with the unmodified curcumin structure significantly enhances its cytotoxic effects [28], regardless of the tumour cell line being tested.

The innovative aspect of this study lies in the identification and characterization of the photosensitizing properties exhibited by these curcumin derivatives. Photoactivation markedly enhanced the cytotoxicity of curcumin and its derivatives AP2961 and AP2975, in both HL-60 and MCF-7 cell lines, as well as of AP2962, which was limited to breast carcinoma cells, thus indicating a promising light-mediated enhancement of their anticancer properties.

Previous investigations employing broad-spectrum visible light have demonstrated that curcumin-mediated photodynamic treatment reduces cell viability in oral squamous carcinoma (HN) cells [44] and cervical carcinoma (HeLa) cells [45]. In the study by Beyer et al., an approximately 50 % increase in lactate dehydrogenase release was observed following treatment with 0.4 μg/mL (1.08 μM) curcumin and subsequent light irradiation, measured 16 h after treatment [44]. Although this effect appears more pronounced than that observed in our experimental conditions, a direct comparison remains difficult due to the lack of information regarding the light intensity and cumulative dose, as well as differences in the viability assay employed. Moreover, Beyer et al. employed significantly lower curcumin concentrations (0.01–1 μg/mL, equivalent to 0.027–2.7 μM) and a shorter pre-irradiation incubation period (1 h) [44], compared to our experimental setting. These differences are determinant, as both the concentration of PS and the duration of incubation before photoactivation are known to affect PS intracellular uptake and subcellular localization [29], thereby influencing curcumin phototoxic effects. Conversely, the study by Banerjee et al. employed

experimental parameters comparable to ours, using a similar curcumin concentration range (0.01–100 μM) and a 4 h incubation period preceding irradiation. An IC_{50} value of 8.2 μM was reported on HeLa cells following a 20 h post-irradiation recovery, using a 1 h visible light exposure at a fluence rate of 2.4 mW/cm^2 and a cumulative dose of 10 J/cm^2 [45]. Notably, despite using a lower cumulative dose (4.32 J/cm^2), we obtained lower IC_{50} values (5.04 and 4.71 μM on HL-60 and MCF-7 cells, respectively). This may reflect differences in the intrinsic sensitivity of the cancer cell lines under investigation [46,47]. Visible light has been proven to enhance curcumin phototoxicity in human bladder (RT112, UMUC3, TCCSUP) [48] and nasopharyngeal carcinoma cells (NPC/CNE2) [49]. However, the lack of information on the specific light wavelength range employed limits the possibility of a direct comparison with our findings.

Visible light irradiation significantly potentiated also the effects of curcumin derivatives AP2961, AP2962, and AP2975, leading to IC_{50} values that were comparable to, or even lower, than those observed for curcumin itself. Among them, AP2975 yielded the most promising results. Indeed, it showed negligible cytotoxicity in HL-60 cells and only mild effects in MCF-7 cells under dark conditions, while light irradiation induced a significant reduction in cell viability in both cell lines. Moreover, AP2975 exhibited a markedly higher PIF compared to curcumin in both cell models, particularly evident in HL-60, indicating a better phototoxic profile compared to the lead compound. Thus, by exhibiting minimal toxicity in the absence of light and becoming significantly cytotoxic only upon photoactivation, AP2975 exemplifies the key characteristics of an ideal PS [50].

PSs are known to damage target cells (*i.e.* cancer cells) through the generation of ROS [51]. A PS, in its ground state (S_0), can absorb a photon (typically in the visible or near-infrared range) and move to a higher-energy singlet excited state (S_1). The excited singlet state (S_1) is usually short-lived, but it can undergo an intersystem crossing to a more stable triplet excited state (T_1). Once in the triplet state, the PS can undergo two main pathways to produce ROS: in the type I mechanism, the excited triplet state interacts directly with molecular oxygen or nearby substrates (like cellular components) via electron or hydrogen atom transfer; this interaction usually produces highly reactive radical ions, such as superoxide anions, hydroxyl radicals, or peroxides [51]; in the type II mechanism, the excited triplet state of the PS transfers its energy directly to molecular oxygen, thus resulting in the generation of singlet oxygen ($^1O_2$), a highly reactive and cytotoxic oxygen form [51]. Our results in cell-free systems showed that the curcumin derivative AP2975, upon irradiation, follow type I mechanism, while the type II mechanism is inactive. This achievement is very interesting and challenging and the search for a new type I organic PS is a highly active area of research for the following reasons: i). type I mechanism is less dependent on molecular oxygen ($^3O_2$) than type II, which requires molecular oxygen to form singlet oxygen ($^1O_2$); ii). type I PSs are more effective in hypoxic (low oxygen) environments, which characterize solid tumors [52]; iii). type I PSs can generate various types of ROS (superoxide radicals, hydroxyl radical, peroxides), resulting in a more extensive or diverse cellular damage [53] and increasing efficacy against cancer cells; iiii). since their mechanism of action involve electron transfer, type 1 PSs can work synergistically with other cancer therapies that exploit redox imbalances in cancer cells [54].

Shifting to in cells experiments, our results also indicate that intracellular ROS do play a critical role in the intoxication paradigm of AP2975. Indeed *o*-phen, which chelates iron ions and blocks Haber-Weiss ROS generation reactions, significantly protected HL-60 cells; moreover, the ROS scavengers BHT and NAC also blunted HL-60 cell death to a similar extent. Notably, NAC pre-incubation also increased cellular thiol levels while the lipophilic antioxidant BHT, which is particularly effective in scavenging organic lipophilic peroxides [55], was slightly more effective than NAC, although the difference was not significant.

Prooxidative conditioning of cells with BSO [56] or ATZ [57] gave apparently contradicting results: while depletion of cellular thiols with BSO markedly reduced the survival of AP2975-treated HL-60 cells, 70 % inhibition of catalase activity with ATZ failed to sensitize cells. The lack of effect of catalase inhibition suggests that H_2O_2 is not generated during AP2975 treatment under light irradiation, and hence is not implicated in the photoactivation cytotoxic pathway. On the contrary, the significant sensitization caused by BSO indicates that the GSSG-GSH cycling driven by the GpX/GR system is likely to play a pivotal role in the detoxification of AP2975-ROS. Differently from catalase, the GpX/GR system is capable of scavenging not only H_2O_2 but also organic peroxides such as *tert*-butyl hydroperoxide or lipid peroxides. The functional relevance of the GpX/GR system is further strengthened by the fact that NAC not only scavenges ROS *per se*, but also increases the levels of the HL-60 sulfhydryl pool, whose availability fuels GpX/GR antioxidant ability. Overall, it can be concluded that photoactivation of AP2975 results in the iron-dependent generation of ROS. Organic peroxides, rather than H_2O_2, are the ROS species likely generated in this process; these organic peroxides are entirely responsible for the photoactivation-dependent AP2975 toxicity. Finally, the lack of any effect by rotenone indicates that the mitochondrial respiratory chain, often contributing to ROS intracellular generation [58], is not involved in the process in question.

Although in cell-free systems, AP2975 ultimately produce peroxides. It is essential to consider that its photodynamic behavior in cells may differ significantly; this is because the intricate biological microenvironment, which includes factors such as oxygen availability, redox-active biomolecules, and cellular context, can lead to the production of different ROS via type I mechanism (i.e. superoxide radicals or hydroxyl radical) or turn on single-electron transfer processes (photoredox catalysis), activating additional pathways [59–61].

PDT triggers a variety of cell death mechanisms, both regulated and accidental, which may occur independently or concurrently, ultimately impacting treatment outcomes [53]. The type of induced cell death is determined by multiple parameters, including the characteristics of the tumor, the physicochemical properties of the PS, its intracellular localization, its accumulation in target tissues, and the dose and duration of light exposure [53]. Apoptosis is the form of PCD most associated with PDT and involves caspase activation, DNA fragmentation, and cleavage of key substrates such as PARP1 [42]. Derivative AP2975 clearly activated apoptotic cell death, as demonstrated by the partial recovery of cell viability upon pre-treatment with the pan-caspase inhibitor zVAD and the increased percentage of cleaved PARP1-positive cells observed after 24 and 48 h from light irradiation. Notably, AP2975 also induced ferroptosis, an iron-dependent form of PCD characterized by the inhibition or downregulation of GPX4, a GSH-dependent enzyme responsible for detoxifying lipid hydroperoxide, whose accumulation consequently leads to cell death [43]. Indeed, AP2975 significantly depleted intracellular GSH levels and reduced GPX4 protein expression. In addition, its phototoxic effects were partially counteracted by Ferr-1. However, the inability of the tested inhibitors to fully restore cell viability suggests the involvement of additional cell-death pathways, including necrosis. Our findings are in line with two recent studies that reported the induction, upon light irradiation, of both apoptosis and ferroptosis by curcumin and an analogue. A study employed a curcumin-loaded nanosystem based on gold nanorods modified with phenylboronic esters and activated by near-infrared (NIR) laser irradiation to achieve a combined photodynamic and photothermal therapy on melanoma cells (A375 and B16) [62]. In the other study, a curcumin analogue featuring 4-diethylamino-phenyl moieties as side aryl rings and retaining the central curcumin scaffold was evaluated in cervical carcinoma (HeLa) cells upon 532 nm laser irradiation. The analogue was specifically designed to localize in lipid droplets and the endoplasmic reticulum. [63]. These findings indicate that the curcumin scaffold can trigger both apoptotic and ferroptotic cell death pathways independently of photoactivation mode and irrespective of the cellular model employed.

Ferroptosis has emerged as a promising alternative cell death

mechanism for eliminating apoptosis-resistant cancer cells [64,65]. Thus, the concurrent induction of both apoptosis and ferroptosis may enhance overall cytotoxicity by targeting a broader spectrum of tumor cells with varying sensitivities to cell death pathways [53]. Overall, our findings suggest that the curcumin derivative AP2975 may serve as a promising PS for PDT since it exhibits a photosensitizing activity comparable to or exceeding that of curcumin. Indeed, photoactivated AP2975 proved to induce oxidative stress and trigger apoptosis, ferroptosis, and necrotic cell death. These multimodal mechanisms of cell death may enhance the phototoxic effects of AP2975 against cancer cells that exhibit differential sensitivity to pro-apoptotic or pro-ferroptotic stimuli. These promising results indicate that further investigations, including *in vivo* studies, are necessary to fully evaluate the therapeutic potential of AP2975 in terms of pharmacokinetics, biodistribution, and safety profile as crucial steps towards translating research from the laboratory to clinical practice.

Funding

The research leading to these results received funding from AIRC under the MFAG 2019 (ID. 22894) project (PI: M.C). G.G. was supported by FIRC-AIRC fellowship for Italy (ID. 26935).

CRediT authorship contribution statement

Carmela Fimognari: Writing – review & editing, Supervision, Funding acquisition, Conceptualization. **Piero Sestili:** Writing – review & editing, Supervision, Conceptualization. **Federica Belluti:** Writing – review & editing, Conceptualization. **Matteo Di Giosia:** Writing – review & editing, Methodology, Investigation, Formal analysis, Data curation. **Francesca Maffei:** Writing – review & editing, Writing – original draft. **Fabio Ferrini:** Writing – review & editing, Methodology, Investigation, Formal analysis, Data curation. **Eleonora Turrini:** Writing – review & editing, Writing – original draft, Methodology, Investigation, Formal analysis, Data curation. **Giulia Greco:** Writing – review & editing, Writing – original draft, Methodology, Investigation, Funding acquisition, Formal analysis, Data curation. **Manuele Di Sante:** Writing – review & editing, Methodology, Investigation, Formal analysis, Data curation. **Matteo Calvaresi:** Writing – review & editing, Supervision, Funding acquisition, Conceptualization. **Giulia Neggiani:** Methodology, Investigation, Formal analysis, Data curation.

Declaration of Competing Interest

The authors declare that they have no known competing financial interests or personal relationships that could have appeared to influence the work reported in this paper.

Data availability

Data will be made available on request.

References

[1] A. Kumar, P N, M. Kumar, A. Jose, V. Tomer, E. Oz, et al., Major phytochemicals: recent advances in health benefits and extraction method, Molecules 28 (2023) 887, https://doi.org/10.3390/molecules28020887.
[2] B.P. George, R. Chandran, H. Abrahamse, Role of phytochemicals in cancer chemoprevention: insights, Antioxidants 10 (2021) 1455, https://doi.org/10.3390/antiox10091455.
[3] M.S. G, M. Swetha, C.K. Keerthana, T.P. Rayginia, R.J. Anto, Cancer chemoprevention: a strategic approach using phytochemicals, Front Pharm. 12 (2022) 809308, https://doi.org/10.3389/fphar.2021.809308.
[4] A. Rudzińska, P. Juchaniuk, J. Oberda, J. Wiśniewska, W. Wojdan, K. Szklener, et al., Phytochemicals in cancer treatment and cancer prevention—review on epidemiological data and clinical trials, Nutrients 15 (2023) 1896, https://doi.org/10.3390/nu15081896.
[5] F. Maggi, Chapter4.18 - turmeric. Nabavi SM, Silva AS, editors. Antioxidants Effects in Health, Elsevier, 2022, pp. 493–504, https://doi.org/10.1016/B978-0-12-819096-8.00007-0.
[6] Y. Peng, M. Ao, B. Dong, Y. Jiang, L. Yu, Z. Chen, et al., Anti-inflammatory effects of curcumin in the inflammatory diseases: status, limitations and countermeasures, DDDT 15 (2021) 4503–4525, https://doi.org/10.2147/DDDT.S327378.
[7] B.M. Razavi, M. Ghasemzadeh Rahbardar, H. Hosseinzadeh, A review of therapeutic potentials of turmeric (Curcuma longa) and its active constituent, curcumin, on inflammatory disorders, pain, and their related patents, Phytother. Res. 35 (2021) 6489–6513, https://doi.org/10.1002/ptr.7224.
[8] S. Hewlings, D. Kalman, Curcumin: a review of its effects on human health, Foods 6 (2017) 92, https://doi.org/10.3390/foods6100092.
[9] K. Jakubczyk, A. Drużga, J. Katarzyna, K. Skonieczna-Żydecka, Antioxidant potential of curcumin—a meta-analysis of randomized clinical trials, Antioxidants 9 (2020) 1092, https://doi.org/10.3390/antiox9111092.
[10] N. Gupta, K. Verma, S. Nalla, A. Kulshreshtha, R. Lall, S. Prasad, Free radicals as a Double-Edged sword: the cancer preventive and therapeutic roles of curcumin, Molecules 25 (2020) 5390, https://doi.org/10.3390/molecules25225390.
[11] Y.-S. Fu, T.-H. Chen, L. Weng, L. Huang, D. Lai, C.-F. Weng, Pharmacological properties and underlying mechanisms of curcumin and prospects in medicinal potential, Biomed. Pharmacother. 141 (2021) 111888, https://doi.org/10.1016/j.biopha.2021.111888.
[12] F. Hassan, M.S. Rehman, M.S. Khan, M.A. Ali, A. Javed, A. Nawaz, et al., Curcumin as an alternative epigenetic modulator: mechanism of action and potential effects, Front Genet 10 (2019) 514, https://doi.org/10.3389/fgene.2019.00514.
[13] T.-J. Liu, S. Hu, Z.-D. Qiu, D. Liu, Anti-Tumor mechanisms associated with regulation of Non-Coding RNA by active ingredients of Chinese medicine: a review, Front Oncol. 10 (2021) 634936, https://doi.org/10.3389/fonc.2020.634936.
[14] R. Farghadani, R. Naidu, Curcumin as an enhancer of therapeutic efficiency of chemotherapy drugs in breast cancer, Int J. Mol. Sci. 23 (2022) 2144, https://doi.org/10.3390/ijms23042144.
[15] N. Dhillon, B.B. Aggarwal, R.A. Newman, R.A. Wolff, A.B. Kunnumakkara, J. L. Abbruzzese, et al., Phase II trial of curcumin in patients with advanced pancreatic cancer, Clin. Cancer Res. 14 (2008) 4491–4499, https://doi.org/10.1158/1078-0432.CCR-08-0024.
[16] S. Hv, J. V Thomas, V. Hs, S. K, An open label, single arm, prospective clinical study to evaluate liver safety and tolerability of PUREMERIC™ (standardized extract from Curcuma longa) in healthy subjects, Toxicol. Rep. 8 (2021) 1955–1959, https://doi.org/10.1016/j.toxrep.2021.11.022.
[17] A.B. Kunnumakkara, D. Bordoloi, G. Padmavathi, J. Monisha, N.K. Roy, S. Prasad, et al., Curcumin, the golden nutraceutical: multitargeting for multiple chronic diseases, Br. J. Pharmacol. 174 (2017) 1325–1348, https://doi.org/10.1111/bph.13621.
[18] L. Xie, X. Ji, Q. Zhang, Y. Wei, Curcumin combined with photodynamic therapy, promising therapies for the treatment of cancer, Biomed. Pharmacother. 146 (2022) 112567, https://doi.org/10.1016/j.biopha.2021.112567.
[19] D. Mundekkad, W.C. Cho, Applications of curcumin and its nanoforms in the treatment of cancer, Pharmaceutics 15 (2023) 2223, https://doi.org/10.3390/pharmaceutics15092223.
[20] K. Gayathri, M. Bhaskaran, C. Selvam, R. Thilagavathi, Nano formulation approaches for curcumin delivery- a review, J. Drug Deliv. Sci. Technol. 82 (2023) 104326, https://doi.org/10.1016/j.jddst.2023.104326.
[21] A. Adeluola, A.H.M. Zulfiker, D. Brazeau, A.R.M.R. Amin, Perspectives for synthetic curcumins in chemoprevention and treatment of cancer: an update with promising analogues, Eur. J. Pharmacol. 906 (2021) 174266, https://doi.org/10.1016/j.ejphar.2021.174266.
[22] R.M.C. Di Martino, A. Bisi, A. Rampa, S. Gobbi, F. Belluti, Recent progress on curcumin-based therapeutics: a patent review (2012-2016). part II: curcumin derivatives in cancer and neurodegeneration, Expert Opin. Ther. Pat. 27 (2017) 953–965, https://doi.org/10.1080/13543776.2017.1339793.
[23] P. Mardaneh, S. Lavian, M. Bagherniya, B.D. Roufogalis, A. Sahebkar, Synthetic curcumin analogs in the treatment of cancer: a literature review, CMC 32 (2025) 3366–3388, https://doi.org/10.2174/0109298673256932231123151626.
[24] W.-B. Zang, H.-L. Wei, W.-W. Zhang, W. Ma, J. Li, Y. Yao, Curcumin hybrid molecules for the treatment of Alzheimer's disease: structure and pharmacological activities, Eur. J. Med. Chem. 265 (2024) 116070, https://doi.org/10.1016/j.ejmech.2023.116070.
[25] E. De Lorenzi, F. Seghetti, A. Tarozzi, L. Pruccoli, C. Contardi, M. Serra, et al., Targeting the multifaceted neurotoxicity of Alzheimer's disease by tailored functionalisation of the curcumin scaffold, Eur. J. Med. Chem. 252 (2023) 115297, https://doi.org/10.1016/j.ejmech.2023.115297.
[26] E. De Lorenzi, D. Franceschini, C. Contardi, R.M.C. Di Martino, F. Seghetti, M. Serra, et al., Modulation of amyloid β-Induced microglia activation and neuronal cell death by curcumin and analogues, IJMS 23 (2022) 4381, https://doi.org/10.3390/ijms23084381.
[27] E. Chainoglou, D. Hadjipavlou-Litina, Curcumin in health and diseases: Alzheimer's disease and curcumin analogues, derivatives, and hybrids, IJMS 21 (2020) 1975, https://doi.org/10.3390/ijms21061975.
[28] F. Seghetti, R.M.C. Di Martino, E. Catanzaro, A. Bisi, S. Gobbi, A. Rampa, et al., Curcumin-1,2,3-Triazole conjugation for targeting the cancer apoptosis machinery, Molecules 25 (2020) 3066, https://doi.org/10.3390/molecules25133066.
[29] J.H. Correia, J.A. Rodrigues, S. Pimenta, T. Dong, Z. Yang, Photodynamic therapy review: principles, photosensitizers, applications, and future directions, Pharmaceutics 13 (2021) 1332, https://doi.org/10.3390/pharmaceutics13091332.

[30] G. Kah, R. Chandran, H. Abrahamse, Curcumin a natural phenol and its therapeutic role in cancer and photodynamic therapy: a review, Pharmaceutics 15 (2023) 639, https://doi.org/10.3390/pharmaceutics15020639.
[31] M.A.G. Marinho, M.D.S. Marques, M.F. Cordeiro, D. De Moraes Vaz Batista Filgueira, A.P. Horn, Combination of curcumin and photodynamic therapy based on the use of redlight or near-infrared radiation in cancer: a systematic review, ACAMC 22 (2022) 2985–2997, https://doi.org/10.2174/1871520622666220425093657.
[32] L.M. Ailioaie, C. Ailioaie, G. Litscher, Latest innovations and nanotechnologies with curcumin as a nature-inspired photosensitizer applied in the photodynamic therapy of cancer, Pharmaceutics 13 (2021) 1562, https://doi.org/10.3390/pharmaceutics13101562.
[33] A. Cantelli, F. Piro, P. Pecchini, M. Di Giosia, A. Danielli, M. Calvaresi, Concanavalin A-rose bengal bioconjugate for targeted gram-negative antimicrobial photodynamic therapy, J. Photochem. Photobiol. B Biol. 206 (2020) 111852, https://doi.org/10.1016/j.jphotobiol.2020.111852.
[34] L. Ulfo, A. Cantelli, A. Petrosino, P.E. Costantini, M. Nigro, F. Starinieri, et al., Orthogonal nanoarchitectonics of M13 phage for receptor targeted anticancer photodynamic therapy, Nanoscale 14 (2022) 632–641, https://doi.org/10.1039/D1NR06053H.
[35] B. Bortot, M. Apollonio, G. Baj, L. Andolfi, L. Zupin, S. Crovella, et al., Advanced photodynamic therapy with an engineered M13 phage targeting EGFR: mitochondrial localization and autophagy induction in ovarian cancer cell lines, Free Radic. Biol. Med. 179 (2022) 242–251, https://doi.org/10.1016/j.freeradbiomed.2021.11.019.
[36] A. Cantelli, M. Malferrari, E.J. Mattioli, A. Marconi, G. Mirra, A. Soldà, et al., Enhanced uptake and phototoxicity of C60@albumin hybrids by folate bioconjugation, Nanomaterials 12 (2022) 3501, https://doi.org/10.3390/nano12193501.
[37] G. Greco, L. Ulfo, E. Turrini, A. Marconi, P.E. Costantini, T.D. Marforio, et al., Light-Enhanced cytotoxicity of doxorubicin by photoactivation, Cells 12 (2023) 392, https://doi.org/10.3390/cells12030392.
[38] A. Marconi, G. Giugliano, M. Di Giosia, T.D. Marforio, M. Trivini, E. Turrini, et al., Identification of blood transport proteins to carry temoporfin: a domino approach from virtual screening to synthesis and in vitro PDT testing, Pharmaceutics 15 (2023) 919, https://doi.org/10.3390/pharmaceutics15030919.
[39] I. Rahman, A. Kode, S.K. Biswas, Assay for quantitative determination of glutathione and glutathione disulfide levels using enzymatic recycling method, Nat. Protoc. 1 (2006) 3159–3165, https://doi.org/10.1038/nprot.2006.378.
[40] H. Aebi, [13] catalase in vitro, in: Methods in Enzymology, 105, Elsevier, 1984, pp. 121–126, https://doi.org/10.1016/S0076-6879(84)05016-3.
[41] I. Shlomovitz, M. Speir, M. Gerlic, Flipping the dogma – phosphatidylserine in non-apoptotic cell death, Cell Commun. Signal 17 (2019) 139, https://doi.org/10.1186/s12964-019-0437-0.
[42] G. Chaitanya, J.S. Alexander, P. Babu, PARP-1 cleavage fragments: signatures of cell-death proteases in neurodegeneration, Cell Commun. Signal 8 (2010) 31, https://doi.org/10.1186/1478-811X-8-31.
[43] B.R. Stockwell, J.P. Friedmann Angeli, H. Bayir, A.I. Bush, M. Conrad, S.J. Dixon, et al., Ferroptosis: a regulated cell death nexus linking metabolism, redox biology, and disease, Cell 171 (2017) 273–285, https://doi.org/10.1016/j.cell.2017.09.021.
[44] K. Beyer, F. Nikfarjam, M. Butting, M. Meissner, A. König, A. Ramirez Bosca, et al., Photodynamic treatment of oral squamous cell carcinoma cells with low curcumin concentrations, J. Cancer 8 (2017) 1271–1283, https://doi.org/10.7150/jca.17176.
[45] S. Banerjee, P. Prasad, A. Hussain, I. Khan, P. Kondaiah, A.R. Chakravarty, Remarkable photocytotoxicity of curcumin in HeLa cells in visible light and arresting its degradation on oxovanadium(iv) complex formation, Chem. Commun. 48 (2012) 7702, https://doi.org/10.1039/c2cc33576j.
[46] A.P. Castano, T.N. Demidova, M.R. Hamblin, Mechanisms in photodynamic therapy: part two-cellular signaling, cell metabolism and modes of cell death, Photo Photo Ther. 2 (2005) 1–23, https://doi.org/10.1016/S1572-1000(05)00030-X.
[47] W. Zhao, L. Wang, M. Zhang, Z. Liu, C. Wu, X. Pan, et al., Photodynamic therapy for cancer: mechanisms, photosensitizers, nanocarriers, and clinical studies, MedComm 5 (2024) e603, https://doi.org/10.1002/mco2.603.
[48] F. Roos, K. Binder, J. Rutz, S. Maxeiner, A. Bernd, S. Kippenberger, et al., The antitumor effect of curcumin in urothelial cancer cells is enhanced by light exposure in vitro, Evid. Based Complement. Altern. Med. 2019 (2019) 1–8, https://doi.org/10.1155/2019/6374940.
[49] H.K. Koon, A.W.N. Leung, K.K.M. Yue, N.K. Mak, Photodynamic effect of curcumin on NPC/CNE2 cells, J. Environ. Pathol. Toxicol. Oncol. 25 (2006) 205–216, https://doi.org/10.1615/JEnvironPatholToxicolOncol.v25.i1-2.120.
[50] S.S. Lucky, K.C. Soo, Y. Zhang, Nanoparticles in photodynamic therapy, Chem. Rev. 115 (2015) 1990–2042, https://doi.org/10.1021/cr5004198.
[51] D.E.J.G.J. Dolmans, D. Fukumura, R.K. Jain, Photodynamic therapy for cancer, Nat. Rev. Cancer 3 (2003) 380–387, https://doi.org/10.1038/nrc1071.
[52] B. Lu, L. Wang, H. Tang, D. Cao, Recent advances in type I organic photosensitizers for efficient photodynamic therapy for overcoming tumor hypoxia, J. Mater. Chem. B 11 (2023) 4600–4618, https://doi.org/10.1039/D3TB00545C.
[53] T. Mishchenko, I. Balalaeva, A. Gorokhova, M. Vedunova, D.V. Krysko, Which cell death modality wins the contest for photodynamic therapy of cancer? Cell Death Dis. 13 (2022) 455, https://doi.org/10.1038/s41419-022-04851-4.
[54] X. Wu, Z. Zhou, K. Li, S. Liu, Nanomaterials-Induced redox imbalance: challenged and opportunities for nanomaterials in cancer therapy, Adv. Sci. 11 (2024) 2308632, https://doi.org/10.1002/advs.202308632.
[55] T. Kaneko, K. Kaji, M. Matsuo, Protection of linoleic acid hydroperoxide-induced cytotoxicity by phenolic antioxidants, Free Radic. Biol. Med. 16 (1994) 405–409, https://doi.org/10.1016/0891-5849(94)90043-4.
[56] O. Cantoni, P. Sestili, A. Guidarelli, F. Cattabeni, Development and characterization of hydrogen preoxide-resistant Chinese hamster overy (CHO) cell variants—II. relationships between non-protein sulfydryl levels and the induction/stability of the oxidant-resistant phenotype, Biochem. Pharmacol. 47 (1994) 1258–1261, https://doi.org/10.1016/0006-2952(94)90398-0.
[57] O. Cantoni, A. Guidarelli, P. Sestili, F. Mannello, G. Gazzanelli, F. Cattabeni, Hydrogen peroxide cytotoxicity under conditions of normal or reduced catalase activity in H2O2-sensitive and -resistant Chinese hamster ovary (CHO) cell variants, Toxicol. Lett. 73 (1994) 193–199, https://doi.org/10.1016/0378-4274(94)90058-2.
[58] P. Sestili, M. Paolillo, M. Lenzi, E. Colombo, L. Vallorani, L. Casadei, et al., Sulforaphane induces DNA single strand breaks in cultured human cells, Mutat. Res. /Fundam. Mol. Mech. Mutagen. 689 (2010) 65–73, https://doi.org/10.1016/j.mrfmmm.2010.05.003.
[59] L. Milla Sanabria, M.E. Rodríguez, I.S. Cogno, N.B. Rumie Vittar, M.F. Pansa, M. J. Lamberti, et al., Direct and indirect photodynamic therapy effects on the cellular and molecular components of the tumor microenvironment, Biochimica et Biophysica Acta (BBA) Reviews Cancer 1835 (2013) 36–45, https://doi.org/10.1016/j.bbcan.2012.10.001.
[60] A.P. Castano, T.N. Demidova, M.R. Hamblin, Mechanisms in photodynamic therapy: part one—photosensitizers, photochemistry and cellular localization, Photo Photodyn. Ther. 1 (2004) 279–293, https://doi.org/10.1016/S1572-1000(05)00007-4.
[61] M. Li, Y. Xu, Z. Pu, T. Xiong, H. Huang, S. Long, et al., Photoredox catalysis May be a general mechanism in photodynamic therapy, Proc. Natl. Acad. Sci. USA 119 (2022), https://doi.org/10.1073/pnas.2210504119.
[62] Y. Zhong, X. Zhang, L. Yang, F. Liang, J. Zhang, Y. Jiang, et al., Hierarchical dual-responsive cleavable nanosystem for synergetic photodynamic/photothermal therapy against melanoma, Materials Science Engineering C 131 (2021) 112524, https://doi.org/10.1016/j.msec.2021.112524.
[63] Y. Wang, X. Li, W. Liu, J. Sha, Z. Yu, S. Wang, et al., A dual organelle-targeting photosensitizer based on curcumin for enhanced photodynamic therapy, J. Mater. Chem. B 11 (2023) 10836–10844, https://doi.org/10.1039/D3TB01648J.
[64] J.P. Friedmann Angeli, D.V. Krysko, M. Conrad, Ferroptosis at the crossroads of cancer-acquired drug resistance and immune evasion, Nat. Rev. Cancer 19 (2019) 405–414, https://doi.org/10.1038/s41568-019-0149-1.
[65] C. Zhang, X. Liu, S. Jin, Y. Chen, R. Guo, Ferroptosis in cancer therapy: a novel approach to reversing drug resistance, Mol. Cancer 21 (2022) 47, https://doi.org/10.1186/s12943-022-01530-y.